

A MODEL OF MAGMA SOLIDIFICATION DURING EXPLOSIVE VOLCANIC ERUPTIONS

A. A. Chernov

UDC 536.421.4:550.3

The paper considers the problem of magma solidification during an explosive volcanic eruption, which is characterized by release of a large amount of gases from the magma. This leads to considerable cooling and, hence, solidification of the magma. It is found that solidified magma has the structure of porous glass with crystalline inclusions.

Key words: volcanic eruption, magma solidification, decompression, gas release, desorption.

Introduction. It is known that volcanic eruptions are very diverse. Thus, the nature of volcanic eruptions can vary from a slow lava flow to a disastrous explosive volcanic eruption, depending on the amount of gases dissolved in magma, which is determined by the depth of the magma chamber. Explosive eruptions are characteristic of high gas-saturated magmas [with a mass fraction of dissolved gases (predominantly water) exceeding 3%].

Since real volcanic eruptions are very difficult to study, simulations of these phenomena are of great importance. It is necessary to adequately describe the magma solidification process during volcanic eruptions because the content of crystalline material in magma has a significant effect on the dynamics of lava flows and, hence, on the structure of the material produced.

There have been a number of studies of the magma solidification process [1–3]. The main disadvantage of these studies is that they consider crystallization in a quasi-isothermal approximation; i.e., it is assumed that supercooling of magma is due only to a change in the effective melting point while the magma temperature remains constant during the entire process. In addition, the mechanisms resulting in magma cooling are not considered and the heat release due to an increase in the crystalline mass per unit volume is ignored.

The present study is an attempt to simulate magma solidification taking into account that the process is nonisothermal.

Formulation of the Problem. The magma flow resulting from an explosive volcanic eruption is characterized by a strong pressure drop (from a few hundreds of megapascals to atmospheric pressure) and, as a consequence, by release of a large amount of gases. This is due to the fact according to Henry's law, the equilibrium concentration of gases dissolved in magma (predominantly water) is a function of pressure P . For water, this dependence has the following form [4]:

$$C^{\text{eq}}(P) = K_{\text{H}}\sqrt{P}.$$

Here C^{eq} is the equilibrium mass concentration of water dissolved in the magma and K_{H} is Henry's constant for water. As the pressure drops, the magma becomes supersaturated and begins to release gas bubbles, which grow as a result of gas diffusion from the melt (up to the time the supersaturation completely disappears). In the present study, magma decompression is considered instantaneous.

As is known, the diffusive growth of a bubble is accompanied by thermal effects. A numerical study of this phenomenon in magmatic melts is performed in [5]. It is shown that magma cooling during degassing is due primarily to energy expenditures in gas desorption from the melt into bubbles. In accordance with this, we estimate the maximum supercooling of magma (relative to the initial temperature) $r_{\text{d}}\Delta C/c_{\text{m}}$ upon release of the entire excess mass of gases [$\Delta C = C^{\text{eq}}(P_{\text{i}}) - C^{\text{eq}}(P_{\text{f}})$] is the supersaturation of the magma due to instantaneous decompression,

Lavrent'ev Institute of Hydrodynamics, Siberian Division, Russian Academy of Sciences, Novosibirsk 630090. Translated from *Prikladnaya Mekhanika i Tekhnicheskaya Fizika*, Vol. 44, No. 5, pp. 79–89, September–October, 2003. Original article submitted March 31, 2003.

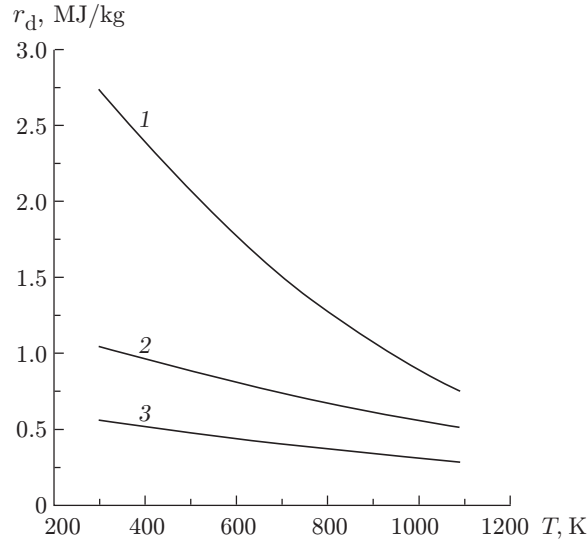


Fig. 1. Heat of water desorption versus temperature for $P = 0.1$ (1); 50 (2), and 100 MPa (3).

P_i and P_f are initial and final pressure, respectively, r_d is the specific heat of desorption, determined according to [6], and c_m is the specific heat of the magma]. We note that the heat of desorption depends on the magma temperature and pressure. The indicated dependence is shown in Fig. 1. Assuming that the initial magma pressure is 170 MPa (which corresponds to a magma chamber depth of approximately 7 km and a mass content of water dissolved in magma of 0.055) and that the final pressure is atmospheric, we find that during degassing, the magma can be cooled by 47 K (ignoring the heat release due to crystallization). When the magma enters the supercooling region, it begins to crystallize.

It should be noted that magma supercooling results not only from its cooling but also from a change in the effective melting point of the magma T_{melt} during degassing, which is determined according to [3] as follows:

$$T_{\text{melt}} = T_{\text{liq}}(1 - X) + T_{\text{sol}}X,$$

$$T_{\text{liq}} = 8.33 \cdot 10^4 C^2 - 139.4 \cdot 10^2 C + 1611.75,$$

$$T_{\text{sol}} = 5.74 \cdot 10^4 C^2 - 98.72 \cdot 10^2 C + 1281.23.$$

Here T_{liq} and T_{sol} are the liquidus and solidus temperatures, C is the mass concentration of gases dissolved in the magma, and X is the volume fraction of the crystalline mass.

In addition to magma crystallization, its amorphization is also possible. Vitrification of the melt occurs because during cooling its temperature becomes lower than the vitrification temperature. The latter is usually determined as the temperature at which the melt viscosity becomes equal to 10^{12} Pa · sec. The temperature dependence of the magma viscosity is described by the Arrhenius dependence [7, 8]

$$\eta = \eta_0 \exp(E_\eta / (k_B T)),$$

where $E_\eta = E_\eta^0(1 - k_\eta C)$ is the activation energy of the viscous flow, E_η^0 is the activation energy for the “dry” melt, k_η is an empirical coefficient, η_0 is a preexponential factor, and k_B is Boltzmann’s constant. Thus, an increase in the magma viscosity results not only from its cooling but also from degassing (because of an increase in the activation energy). Figure 2 shows the vitrification temperature of the magma and the liquidus and solidus temperatures versus the mass concentration of gases dissolved in the magma. The vitrification temperature was calculated for the following kinetic parameters of the magma: $E_\eta^0 = 5.06 \cdot 10^{-19}$ J/mole, $\eta_0 = 10^{-2.5}$ Pa · sec, and $k_\eta = 11$.

Let us estimate the heat effects accompanying the growth of a single bubble formed at the initial time in the melt under instantaneous nucleation conditions.

Solution of the Thermal Problem in the Case of Growth of a Single Bubble. We shall consider the problem of magma cooling during diffusive growth of a single bubble. The problem reduces to solving the boundary-value problem for the heat-conduction equation

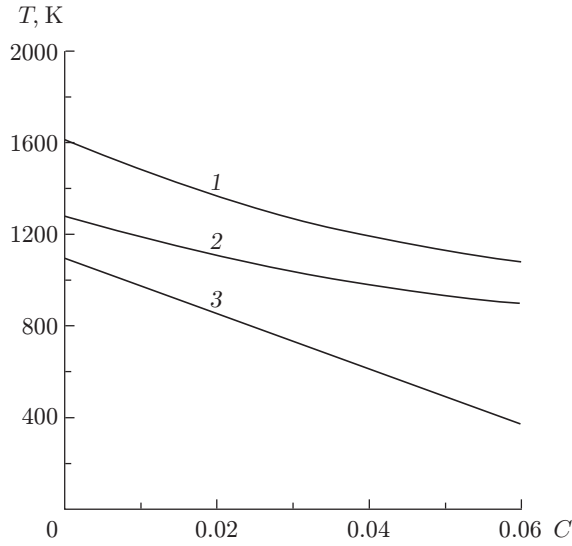


Fig. 2. Liquidus (1) and solidus (2) temperatures and vitrification temperature (3) versus mass concentration of gases dissolved in magma.

$$\frac{\partial T}{\partial t} + v \frac{\partial T}{\partial r} = a_m \left(\frac{2}{r} \frac{\partial T}{\partial r} + \frac{\partial^2 T}{\partial r^2} \right) \quad (1)$$

subject to the initial condition

$$T = T_0 \quad \text{at} \quad t = 0 \quad (2)$$

and the boundary conditions

$$-\lambda_m \frac{\partial T}{\partial r} = -\rho_m r_d D \frac{\partial C}{\partial r} \quad \text{at} \quad r = R_b, \quad T \rightarrow T_0 \quad \text{at} \quad r \rightarrow \infty. \quad (3)$$

Here T is the temperature of the melt, T_0 is the initial temperature of the melt (below, it is considered equal to the melting point of the melt T_{melt} at the initial time), ρ_m is the density of the melt, a_m and λ_m are the thermal diffusivity and thermal conductivity of the melt, respectively, D is the gas diffusivity in the melt, and R_b is the bubble radius. The dependence of the velocity of the melt away from the bubble is obtained from the continuity equation $v(r) = v_b R_b^2 / r^2$, where $v_b = \dot{R}_b$ is the bubble growth rate.

The problem (1)–(3) must be supplemented by the time dependence of the bubble radius that follows from the solution of the problem of bubble growth in a supersaturated solution.

The present problem was studied in [9, 10], in which two stages of growth of a single bubble are distinguished. At the initial stage of the growth, the bubble pressure is kept equal to its initial value (before the moment of decompression) and the bubble growth is limited by viscous stresses. The bubble pressure gradually decreases and eventually becomes equal to ambient pressure. The bubble growth rate at this stage is determined primarily by diffusion. In this case, we obtain the quasisteady-state solution of the problem

$$R_b(t) = \sqrt{D_{\text{eff}} t}, \quad D_{\text{eff}} = 2D\rho_m \Delta C / \rho_g, \quad (4)$$

where ρ_g is the density of the bubble gas, determined from the ideal gas equation of state. The gas flow into the bubble is determined from the expression

$$\left. \frac{\partial C}{\partial r} \right|_{r=R_b} = \frac{\Delta C}{R_b}. \quad (5)$$

According to the results of [10], the time of establishment of a quasisteady-state concentration profile depends primarily on the initial gas content, which determines the viscosity of the magma. Thus, during bubble growth in a highly gas-saturated magma ($\eta < 10^6$ Pa \times sec and $\Delta P \approx 10^8$ Pa), a quasisteady-state concentration profile is established at $t < 0.01$ sec. A different situation arises for gas release from low gas-saturated magmas ($\eta > 10^8$ Pa \cdot sec and $\Delta P \approx 10^6$ Pa), where transition to the asymptotic bubble-growth law occurs at $t > 1000$ sec.

As is noted above, in the present paper, we consider the case of highly gas-saturated magmas, for which the square root law of bubble growth (4) is valid practically from the initial time. In this case, the problem (1)–(3) has a self-similar solution.

We introduce the variable $\gamma = \hat{r}/\sqrt{a_m t}$ ($\hat{r} = r - R_b$ is a coordinate related to the front of the bubble). Then, by virtue of (4) and (5), the heat-conduction equation (1) reduces to the ordinary differential equation

$$\theta'' + f(\gamma)\theta' = 0, \quad (6)$$

where $f(\gamma) = (1/2)[\gamma + \sqrt{\text{Le}^*}(1 - \text{Le}^*/(\gamma + \sqrt{\text{Le}^*})^2)] + 2/(\gamma + \sqrt{\text{Le}^*})$, $\text{Le}^* = D_{\text{eff}}/a_m$ is a modified Lewis number, and $\theta = (T - T_0)/T_0$ is the dimensionless temperature. Boundary conditions (3) are written as

$$\theta' = \varkappa \quad \text{at} \quad \gamma = 0, \quad \theta = 0 \quad \text{at} \quad \gamma \rightarrow \infty, \quad (7)$$

where $\varkappa = \rho_m r_d D \Delta C / (\lambda_m T_0 \sqrt{\text{Le}^*})$.

For $\text{Le}^* \ll 1$, characteristic of the problem considered, an approximate solution of Eq. (6) can be obtained with allowance for boundary conditions (7):

$$\theta(\gamma) \simeq -\varkappa \text{Le}^* \left(\frac{\exp[-(\gamma + \sqrt{\text{Le}^*})^2/4]}{\gamma + \sqrt{\text{Le}^*}} + \frac{\sqrt{\pi}}{2} \text{erfc} \frac{\gamma + \sqrt{\text{Le}^*}}{2} \right). \quad (8)$$

From solution (8) it follows that the maximum supercooling of the melt $\Delta T = T_0 - T$ is reached at the front of the bubble ($\gamma = 0$) and remains constant during the entire process:

$$\Delta T \Big|_{r=R_b} \simeq \rho_m r_d D \Delta C / \lambda_m.$$

Calculations yield low values of magma supercooling at the front of the bubble: $\Delta T|_{r=R_b} \approx 0.15$ K at $\Delta C \approx 0.055$. The calculation was conducted for the following thermal and kinetic parameters of magma: density $\rho_m = 2300$ kg/m³, thermal diffusivity $a_m = 1.47 \cdot 10^{-7}$ m²/sec, specific heat $c_m = 1.35 \cdot 10^3$ J/(kg · K), diffusivity $D = 2 \cdot 10^{-11}$ m²/sec, Henry's constant $K_H = 4.33 \cdot 10^{-6}$ Pa^{-1/2}, and specific heat of crystallization $L = 1.4 \cdot 10^5$ J/kg. The low values of melt supercooling are due to the fact that the Lewis numbers characteristic of the present problem are much smaller than unity ($\text{Le}^* = 0.1\text{--}0.2$). This implies that the thermal wave propagates much faster than the diffusion wave. Thus, the growth of a single bubble does not lead to a significant supercooling of the melt, and hence, to its crystallization. Therefore, one needs to consider the problem of magma solidification during growth of an ensemble of gas bubbles. The temperature field over the entire volume of the melt can be considered uniform and varying with time owing to the presence of internal heat sources in the melt. A solution of the present problem is given below.

Solution of the Problem of Melt Solidification During Growth of an Ensemble of Gas Bubbles.

We consider the problem of magma solidification during propagation of an ensemble of gas bubbles. The problem reduces to considering a bounded volume of magma with internal heat sources determined by gas desorption from the melt into bubbles and crystallization of the melt using the kinetic theory of phase transitions. We write the heat-conduction equation taking into account that at each time, the temperature field is uniform over the entire volume of the melt:

$$\rho_m c_m \frac{dT}{dt} = -Q_d + Q_{\text{cr}}. \quad (9)$$

Here T is the melt temperature averaged over the volume, $Q_d = r_d J_D$ is the amount of heat expended in gas desorption per unit volume, J_D is the total diffusion gas flow from the melt into bubbles per unit volume, $Q_{\text{cr}} = \rho_m L(dX/dt)$ is the heat released per unit volume by growing nuclei of the new phase due to crystallization, $X = V(t)/V$ is the volume fraction of the crystalline mass in the melt, V is the sample volume, $V(t)$ is the volume occupied by the crystalline phase, and L is the specific heat of crystallization.

Assuming that the bubble nucleation process is instantaneous and the bubble concentration per unit volume is constant during the entire process, we write the expression for the diffusion gas flow in the bubbles:

$$J_D = N_b \frac{dm_b}{dt}, \quad (10)$$

where N_b is the number of bubbles per unit volume formed during nucleation (in the calculations, the number of bubbles per unit volume is set equal to $10^{13}\text{--}10^{14}$ m⁻³, which corresponds to the number of bubbles in volcanic glass and pumice), and m_b is the mass of a bubble determined from the relation

$$\frac{dm_b}{dt} = 4\pi R_b^2 \rho_m D \left. \frac{\partial C}{\partial r} \right|_{r=R_b}.$$

As in the previous calculations, we use the quasisteady-state solution of the diffusive problem of growth of a single bubble in a supersaturated solution [see (4) and (5)]. In the case of growth of an ensemble of gas bubbles, this solution with is valid high accuracy up to the moment the diffusion layers of neighboring bubbles begin to interact. Bubble growth ceases after the excessive gas that appeared in the melt as a result of decompression is released into the gas phase. It is easy to obtain the limiting radius R_b^f of a single bubble:

$$R_b^f = \left(\frac{3}{4\pi N_b} \frac{\rho_m}{\rho_g} \Delta C \right)^{1/3}.$$

Let us consider the dynamics of melt crystallization upon cooling. It is known that nuclei of the new phase arise in the volume of the melt as a result of fluctuation, and their formation is possible on both impurity particles (heterogeneous nucleation) and in the absence of impurities (homogeneous nucleation). According to the estimates given in [11], the contribution of homogeneous nucleation to mass crystallization for fairly pure melts becomes predominant only at cooling rates higher than 10^6 K/sec. The cooling rate of magma during degassing is much lower than this value, 1–2 K/sec. In addition, the work of formation of a critical nucleus for the characteristic magma supercooling has a large value (approximately $500k_B T$), while intense nucleation is characterized by an energy barrier of $(30\text{--}80)k_B T$. Therefore, in considering the problem of magma solidification, it is necessary to use the theory of heterogeneous nucleation.

According to this theory, the frequency of heterogeneous nucleation J^{het} in an unsteady nonisothermal process is given by the expression [11]

$$J^{\text{het}}(t) = J_s^{\text{het}} \exp\left(-\frac{t_0}{t_e}\right), \quad J_s^{\text{het}} = \sum_{i=1}^{N_{\text{cr}}} n_i B \exp\left(-\frac{W_* \psi(\varphi_i)}{k_B T}\right). \quad (11)$$

Here J_s^{het} is the steady-state frequency of heterogeneous nucleation corresponding to a steady-state phase transition ($t_e \gg t_0$); $t_0 \simeq n_*^{4/3} (h/(k_B T)) \exp(E_\eta/(k_B T))$ is the characteristic time of establishment of steady-state nucleation (delay time); h is Planck's constant; n_* is the number of molecules in a critical nucleus (the radius of a critical nucleus for homogeneous nucleation is defined by the expression $R_* = 2\sigma_{ls} T_{\text{melt}}/(\rho_m L \Delta T)$; σ_{ls} is the surface tension on the melt–crystal interface; the heterogeneous nucleation model uses the same curvature radius of the surface of a dome-shaped nucleus as for homogeneous nucleation); the parameter $t_e = t_0(T) \int_0^t t_0(T)^{-1} dt$ characterizes the age

of the sample in a nonisothermal process (in the case of an isothermal process, $t_e = t$, i.e., the characteristic age of the sample is equal to the time of observation); $B = 2 d_m (\sigma_{ls}/(k_B T))^{1/2} (k_B T/h) \exp(-E_\eta/(k_B T))$ is a kinetic coefficient; d_m is the characteristic molecular diameter, $W_* = 16\pi \sigma_{ls}^3 T_{\text{melt}}^2 / (3\rho_m^2 L^2 \Delta T^2)$ is the work of formation of a critical nucleus in a homogeneous process, $\psi(\varphi_i) = (1/4)(1 - \cos \varphi_i)^2 (2 + \cos \varphi_i)$, φ_i is the equilibrium surface wetting angle for the i th impurity particle (generally speaking, impurity particles are characterized by different wetting angles; the angle $\varphi = \pi$ corresponds to the case of homogeneous nucleation); n_i is the number of molecules on the surface of the i th impurity particle that can become nuclei (for homogeneous nucleation, it is usually assumed that any molecule of the melt can become a nucleus); and N_{cr} is the number of impurity particles per unit volume of the melt. It should be noted that the establishment of a steady-state nucleation process can be significantly retarded because of a high magma viscosity (and, hence, a large delay), which, in addition, increases during gas release.

From expression (11) it follows that an a priori description of heterogeneous nucleation is considerably hampered because of a large number of random and poorly studied factors. In particular, formula (11) contains parameters that are difficult to determine, such as surface tension on the melt–crystal interface σ_{ls} (which varies from 0.35 to 0.5 J/m² depending on the magma composition), the surface wetting angle for an impurity particle φ , etc. It should be noted that with decrease in the wetting angle, the work of formation of a critical nucleus on the surface decreases rapidly, as well as the delay time. In practice, this leads to the formation of crystallization nuclei predominantly on active impurity particles. In the case of almost complete wetting ($\varphi \rightarrow 0$), crystallization on the surface should begin under practically zero supercooling. In the present paper, we restrict ourselves to the case of heterogeneous nucleation on well-wettable impurity particles. In this case, the nucleation of the crystalline phase can be considered instantaneous. The time dependence of the fraction of the crystallized volume is defined by the expression [12]

$$X(t) = N_{\text{cr}} \frac{4\pi}{3} \left(\int_0^t v_{\text{cr}}(\tau) d\tau \right)^3, \quad (12)$$

where $v_{\text{cr}} = \dot{R}_{\text{cr}}$ is the crystal growth rate, R_{cr} is the radius of the crystal, and N_{cr} is the number of supercritical crystalline nuclei formed on active impurity particles at the initial time.

The crystal growth rate is defined according to [13, 14]:

$$v_{\text{cr}} = d_{\text{m}} \frac{k_{\text{B}} T_{\text{f}}}{h} \exp\left(-\frac{E_{\eta}}{k_{\text{B}} T_{\text{f}}}\right) \left[1 - \exp\left(-\frac{\rho_{\text{m}} L \Delta T_{\text{f}}}{N k_{\text{B}} T_{\text{f}} T_{\text{melt}}}\right)\right]. \quad (13)$$

Here $\Delta T_{\text{f}} = T_{\text{melt}} - T_{\text{f}}$ is the supercooling at the crystallization front, T_{f} is the melt temperature at the crystallization front, which, generally speaking, differs from the melt temperature away from the front because the latent heat of phase transition releases during crystal growth.

For small supercoolings, expression (13) can be written as

$$v_{\text{cr}} = K \Delta T_{\text{f}}, \quad (14)$$

where $K = d_{\text{m}} \rho_{\text{m}} L \exp(-E_{\eta}/(k_{\text{B}} T_{\text{f}}))/(N h T_{\text{melt}})$ is a kinetic coefficient that characterizes the frequency of addition of molecules from the melt to the crystal. The quantity v_{cr} , defined by expression (14), is the first term of series (13) for small ΔT_{f} . The mechanism of crystal growth governed by the law (14) is called the normal mechanism.

The question as to how the temperature at the crystallization front T_{f} varies with time remains open.

Following [15], we consider the following problem. Let a spherical crystal grow in the melt at temperature $T_{\infty} < T_{\text{melt}}$. The temperature field around the crystal can be approximately described by the steady-state heat-conduction equation

$$\frac{d^2 T}{dr^2} + \frac{2}{r} \frac{dT}{dr} = 0. \quad (15)$$

Since $T \rightarrow T_{\infty}$ as $r \rightarrow \infty$, the solution of Eq. (15) is written as

$$T(r) = T_{\infty} - (T_{\infty} - T_{\text{f}}) R_{\text{cr}}/r. \quad (16)$$

The boundary conditions on the crystal surface include the heat-balance equation

$$\rho_{\text{m}} L v_{\text{cr}} = -\lambda_{\text{m}} \left. \frac{\partial T}{\partial r} \right|_{r=R_{\text{cr}}} \quad (17)$$

and Eq. (14), describing the kinetics of the phase transition.

Substituting Eq. (16) into (17) and eliminating the unknown function T_{f} from the system obtained, we have the equation

$$(\rho_{\text{m}} L / \lambda_{\text{m}}) R_{\text{cr}} v_{\text{cr}} + (1/K) v_{\text{cr}} = \Delta T. \quad (18)$$

We note that the right side of Eq. (18) represents the supercooling of the melt away from the crystallization front. In the case $\Delta T = \text{const}$, Eq. (18) can be integrated:

$$v_{\text{cr}} = K \Delta T (1 + (2\rho_{\text{m}} L K^2 / \lambda) \Delta T t)^{-1/2}, \quad (19)$$

$$T_{\text{f}} = T_{\text{melt}} - \Delta T (1 + (2\rho_{\text{m}} L K^2 / \lambda) \Delta T t)^{-1/2}.$$

From Eq. (19) it follows that for $t \ll \lambda_{\text{m}} / (2\rho_{\text{m}} L K^2 \Delta T)$, the crystallization is an isothermal process ($T_{\text{f}} = T_{\infty}$) and the crystal growth rate is defined by the phase-transition kinetics: $v_{\text{cr}} = K \Delta T$. At large times, heat is accumulated near the surface of the growing nucleus, and eventually, the crystal surface temperature becomes equal to the melting point ($T_{\text{f}} = T_{\text{melt}}$). In this case, heat release becomes the predominant factor in the crystallization process. Because the magma viscosity is high (and, as a consequence, the kinetic coefficient K is small), the time of attainment a regime in which the crystallization process is determined by heat release is much larger than the characteristic time of magma degassing. Therefore, the process of crystal growth in the magma is considered isothermal ($T_{\text{f}} = T_{\infty}$).

Equation (9) combined with expressions (10) and (12) completely defines the dynamics of magma crystallization, i.e., the time dependence of the volume fraction of the crystalline mass.

We calculated the process of solidification of a highly gas-saturated magma after instantaneous decompression. The thermal and kinetic parameters of the magma used in the calculations are given above. The initial mass concentration of water dissolved in the magma was set equal to 0.055, and the number of bubbles per unit volume

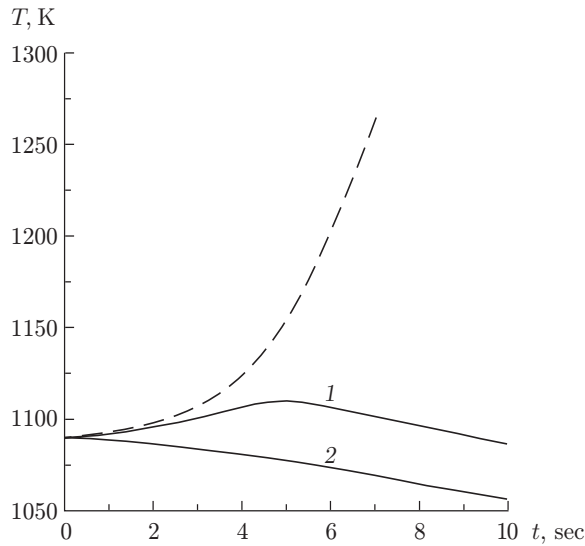


Fig. 3. Magma temperature versus time taking into account (1) and ignoring (2) crystallization for $N_{cr} = 10^{13} \text{ m}^{-3}$ (the dashed curve is the effective melting point of the magma).

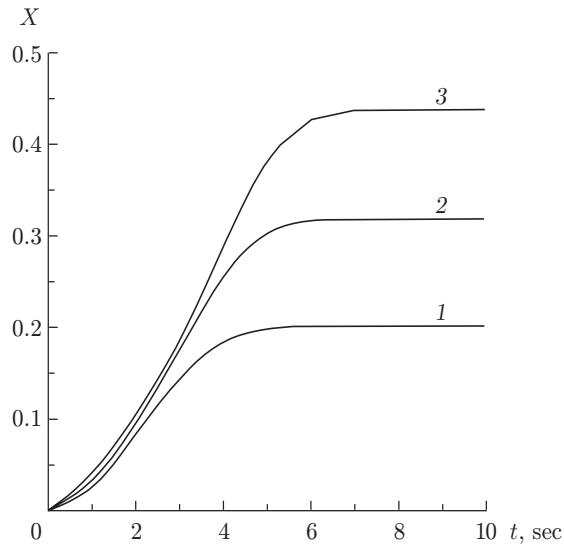


Fig. 4. Volume fraction of the crystalline mass versus time for $N_{cr} = 10^{11}$ (1), 10^{13} (2), 10^{15} m^{-3} (3).

is $4 \cdot 10^{13}$, which corresponds to the number of bubbles in volcanic glass and pumice. The number of supercritical crystalline nuclei, which depends primarily on the structure of the magma (number of active impurity particles), was varied from 0 to 10^{15} m^{-3} .

Figure 3 shows the magma temperature during its degassing versus time taking into account and ignoring crystallization. It is obvious that the heat release due to an increase in the crystalline mass leads to a significant change in the cooling dynamics. The dashed curve shows the effective melting point of the magma. It is evident that its increase is caused mainly by a decrease in the concentration of gases dissolved in magma due to magma degassing.

Figure 4 shows the volume fraction of the crystalline mass versus time. It is evident that it increases considerably at the initial stage of the process. However, the growth rate gradually decreases and, eventually, becomes nearly equal to zero. This is due to the fact that during degassing and cooling, the magma viscosity strongly increases (from 10^3 to $10^{12} \text{ Pa} \cdot \text{sec}$) and, accordingly, the value of the kinetic coefficient K , determining the crystal growth rate, considerably decreases. Even at $t \approx 6 \text{ sec}$, the structure of the magma resembles a gelatinous

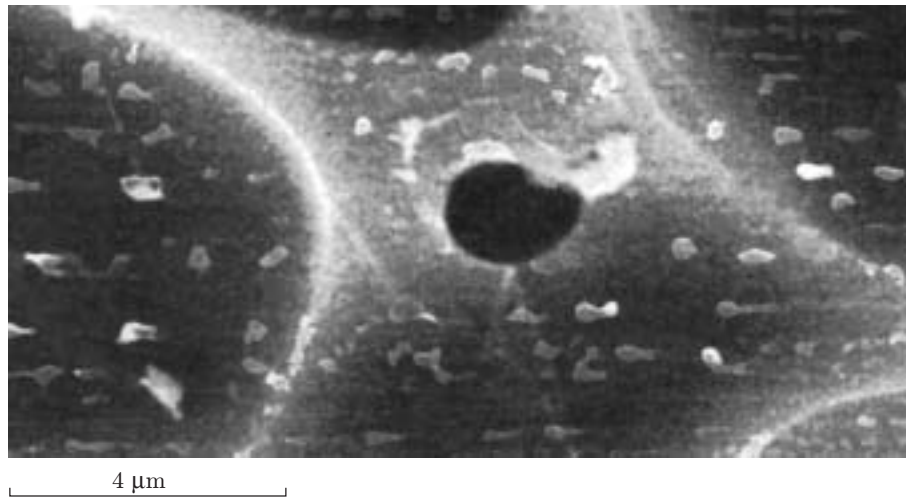


Fig. 5. Structure of pumice.

fluid with crystal grains “frozen” in it; the volume fraction of the crystal grains reaches 40% depending on the number of supercritical nuclei in the volume of the melt at the initial time. As a result, when almost the entire mass of the gas is released from the magma, the magma viscosity approaches 10^{12} Pa·sec; i.e., uncrystallized magma enters a glasslike state. If the active crystallization nuclei are small in number, the magma becomes completely amorphous.

The volume fraction of bubbles at the end of the gas-release process can also be found. From calculations performed for the problem parameters considered, it is 60%. The average diameter of a bubble is approximately equal to $30 \mu\text{m}$.

The simulated structure of solidified magma corresponds both qualitatively and quantitatively to the structure of real pumice (Fig. 5).

Conclusions. The problem of magma solidification during an explosive volcanic eruption was considered. The thermal effects accompanying the growth of a single bubble are analyzed. A self-similar solution of the thermal problem is found for the asymptotic growth law. It is shown that supercooling is established at the front of the bubble and remains constant during the entire process, but, for the characteristic parameters of the problem considered, it is insufficient for melt crystallization. Therefore, the problem of magma solidification during growth of an ensemble of gas bubbles is considered. The volume fraction of the crystalline mass is shown to considerably increase at the initial stage of gas release. In the process of magma degassing, its viscosity strongly increases and the crystal growth rate considerably decreases and eventually becomes nearly equal to zero; as a result, the growth of the crystalline mass ceases. After release of the almost entire mass of the gas, the solidified magma is shown by analysis to be glass containing crystal grains with a volume fraction of 40% and “frozen” bubbles about $30 \mu\text{m}$ in diameter with a volume fraction of 60%.

The author thanks V. K. Kedrinskii for useful discussions.

This work was supported by the INTAS (Grant No. 01-0106).

REFERENCES

1. M. Hort, “Abrupt change in magma liquidus temperature because of volatile loss or magma mixing: effects on nucleation, crystal growth and thermal history of the magma,” *J. Petrol.*, **39**, No. 5, 1063–1076 (1998).
2. O. E. Melnik and R. S. J. Sparks, “Nonlinear dynamics of lava dome extrusion,” *Nature*, **402**, No. 4, 37–41 (1999).
3. O. E. Melnik, “Unsteady model of the dynamics of volcanic eruptions taking into crystallization and gas filtration through the magma,” *Dokl. Ross. Akad. Nauk SSSR*, **377**, No. 7, 629–633 (2001).
4. E. Stolper, “Water in silicate glasses: an infrared spectroscopic study,” *Contrib. Mineral. Petrol.*, **81**, 1–17 (1982).
5. A. A. Proussevitch and D. L. Sahagian, “Dynamics and energetics of bubble growth in magmas: Analytical formulation and numerical modeling,” *J. Geophys. Res.*, **103**, No. B8, 18223–18251 (1998).

6. A. A. Proussevitch and D. L. Sahagian, "Dynamics of coupled diffusive and decompressive bubble growth in magmatic systems," *J. Geophys. Res.*, **101**, No. 8, 17447–17456 (1996).
7. E. S. Persikov, V. A. Zharikov, P. G. Bukhtiyarov, and S. F. Pol'skoy, "The effect of volatiles on the properties of magmatic melts," *Europ. J. Mineral.*, **2**, 621–642 (1990).
8. E. S. Persikov, "The viscosity of magmatic liquids: experiment, generalized patterns. A model for calculation and prediction. Applications," in: *Physical Chemistry of Magmas*, Vol. 9: *Advances in Physical Geochemistry*, Springer-Verlag, New York (1991), pp. 1–40.
9. V. Lyakhovsky, S. Hurwitz, and O. Navon, "Bubble growth in rhyolitic melts: Experimental and numerical investigation," *Bull. Volcanol.*, **58**, No. 1, 19–32 (1996).
10. O. Navon, A. Chekhir, and V. Lyakhovsky, "Bubble growth in highly viscous melts: theory, experiments, and autoexplosivity of dome lavas," *Earth Planet. Sci. Lett.*, **16**, 763–776 (1998).
11. V. P. Skripov and V. P. Koverda, *Spontaneous Crystallization of Supercooled Fluids* [in Russian], Nauka, Moscow (1984).
12. A. N. Kolmogorov, "Statistical theory of metal crystallization," *Izv. Akad. Nauk SSSR, Ser. Mat.*, **3**, 355–359 (1937).
13. D. R. Uhlmann, "A kinetic treatment of glass formation," *J. Non-Cryst. Solids*, **7**, No. 2, 337–348 (1972).
14. H. A. Davies, "The formation of metallic glasses," *Phys. Chem. Glasses*, **17**, No. 5, 159–173 (1976).
15. B. Ya. Lyubov, *Theory of Crystallization in Large Volumes* [in Russian], Nauka, Moscow (1975).